

Electronic Supplementary Material (ESI) for CrystEngComm.
This journal is © The Royal Society of Chemistry 2017

Supporting Information

Site occupancy and photoluminescence tuning of $\text{La}_3\text{Si}_6\text{-}_x\text{Al}_x\text{N}_{11-x/3}\text{:Ce}^{3+}$ phosphors for high power white light-emitting diodes

Fu Du^a, Weidong Zhuang^{a,†}, Ronghui Liu^{a,†}, Jiyou Zhong^b,
Yuanhong Liu^a, Yunsheng Hu^a, Wei Gao^a, Xia Zhang^a, Lei Chen^a,
Kun Lin^c

^a National Engineering Research Center for Rare Earth Materials, General Research Institute for Nonferrous Metals, and Grirem Advanced Materials Co., Ltd., Beijing 100088, PR China

^b School of Physics and Optoelectronic Engineering, Guangdong University of Technology, Guangzhou 510006, PR China.

^c University of Science & Technology Beijing, Beijing 100083, China

† E-mail: wdzhuang@126.com (W.D. Zhuang), griremlrh@126.com (R.H. Liu)

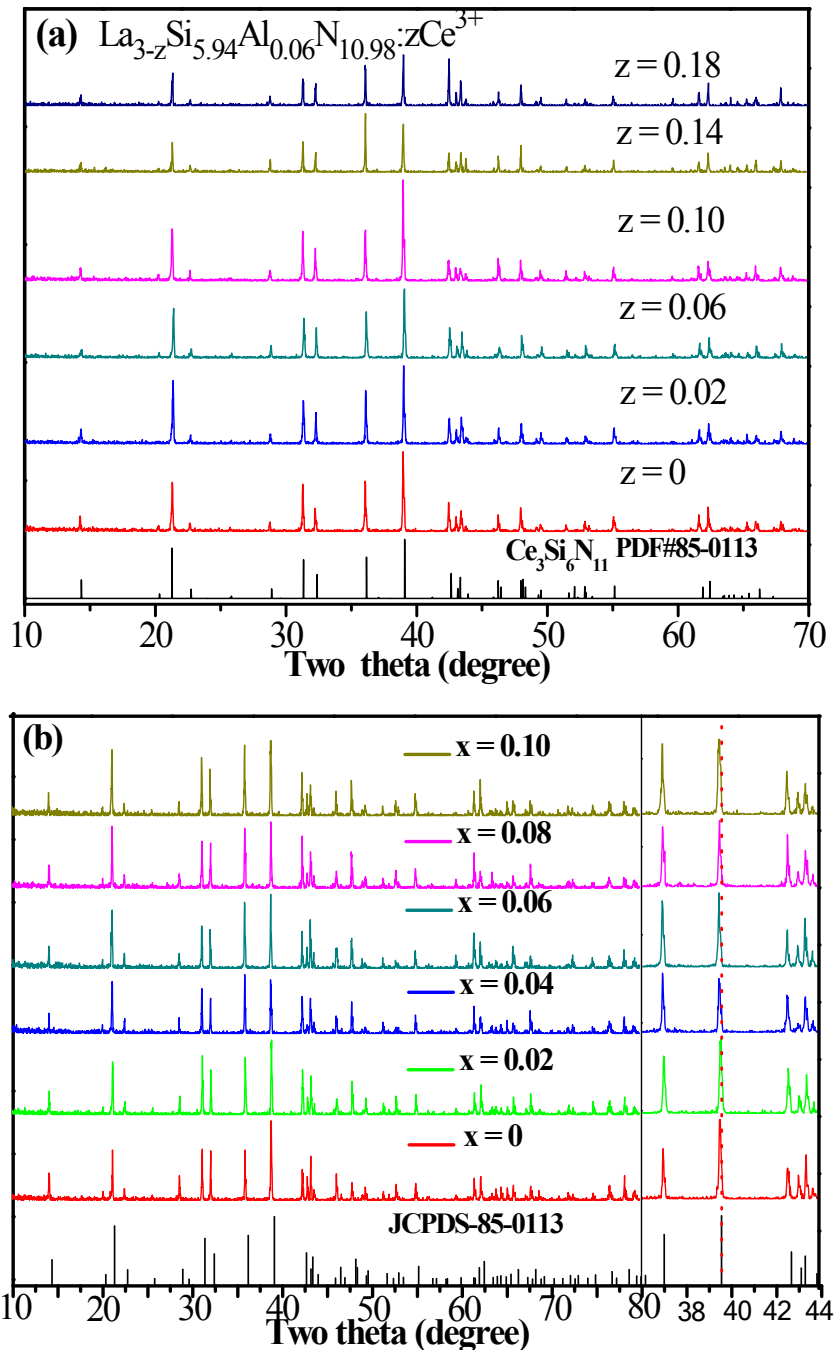


Fig. S1 XRD patterns of $\text{La}_{3-z}\text{Si}_{5.94}\text{Al}_{0.06}\text{N}_{10.98}:z\text{Ce}^{3+}$ ($z = 0, 0.02, 0.06, 0.10, 0.14, 0.18$) (a), $\text{La}_{2.86}\text{Si}_{6-x}\text{Al}_x\text{N}_{11-x/3}:0.14\text{Ce}^{3+}$ ($x = 0, 0.02, 0.04, 0.06, 0.08$ and 0.1) (b).

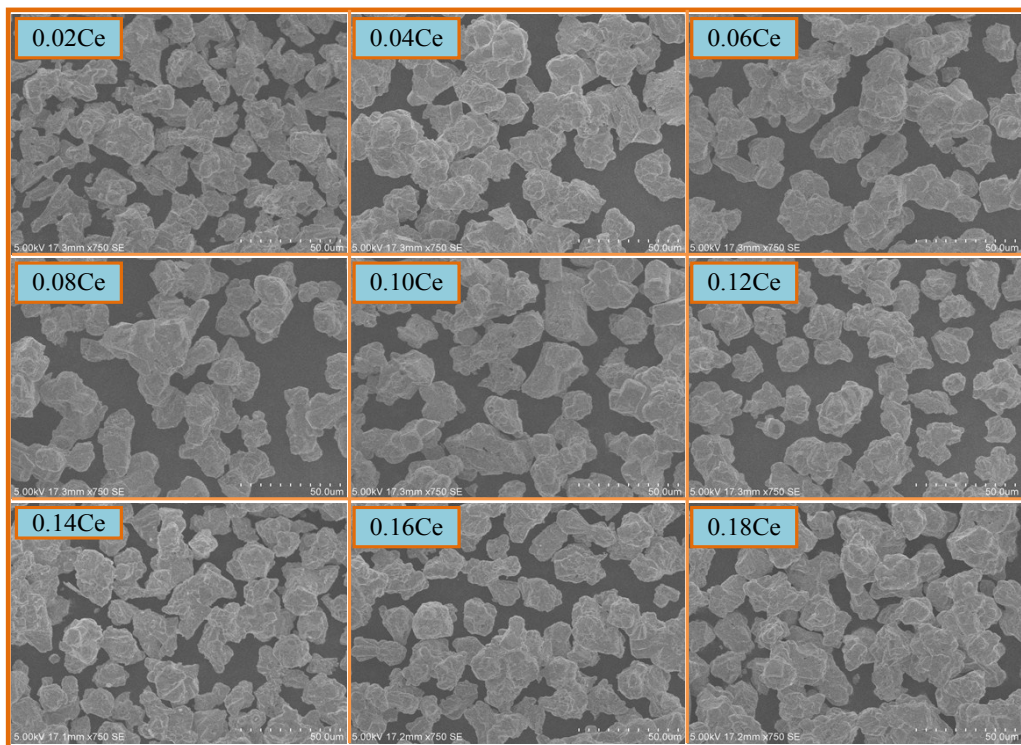
Table S1. EDS elemental composition analysis of $\text{La}_{2.86}\text{Si}_{6-x}\text{Al}_x\text{N}_{11-x/3}:0.14\text{Ce}^{3+}$ sample with $x = 0.1$.

Element	Atomic%	
	Point 1	Point 2
La	21.34	28.04
Si	38.95	46.68
Al	0.64	0.67
Atom Si/Al	0.0164	0.144
Atom Si/Al theory ratio	0.017	

Table S2. Selected crystallographic parameters from Rietveld refinement for the $\text{La}_{2.86}\text{Si}_{6-x}\text{Al}_x\text{N}_{11-x/3}:0.14\text{Ce}^{3+}$ ($x = 0, 0.02, 0.04, 0.06, 0.08$ and 0.1) samples.

atomic occupancy in $\text{La}_{2.86}\text{Si}_{6-x}\text{Al}_x\text{N}_{11-x/3}:0.14\text{Ce}^{3+}$					
$x = 0$	$x = 0.02$	$x = 0.04$	$x = 0.06$	$x = 0.08$	$x = 0.1$
$\text{La}_{(1)}$	0.99	0.993	0.976	0.92	0.863
$\text{Ce}_{(1)}$	0.01	0.007	0.026	0.08	0.137
$\text{La}_{(2)}$	0.85	0.858	0.869	0.875	0.874

$\text{Ce}_{(2)}$	0.15	0.142	0.131	0.125	0.126	0.121
$\text{Si}_{(1)}$	1	0.88	0.876	0.872	0.869	0.863
$\text{Al}_{(1)}$	0	0.120	0.124	0.128	0.131	0.137
$\text{Si}_{(2)}$	1	1	1	1	1	1
$\text{Al}_{(2)}$	0	0	0	0	0	0
$\text{N}_{(1)}$	1	1	1	1	1	1
$\text{N}_{(2)}$	1	1	1	1	1	1
$\text{N}_{(3)}$	1	1	1	1	1	1
$\text{N}_{(4)}$	1	1	1	1	1	1



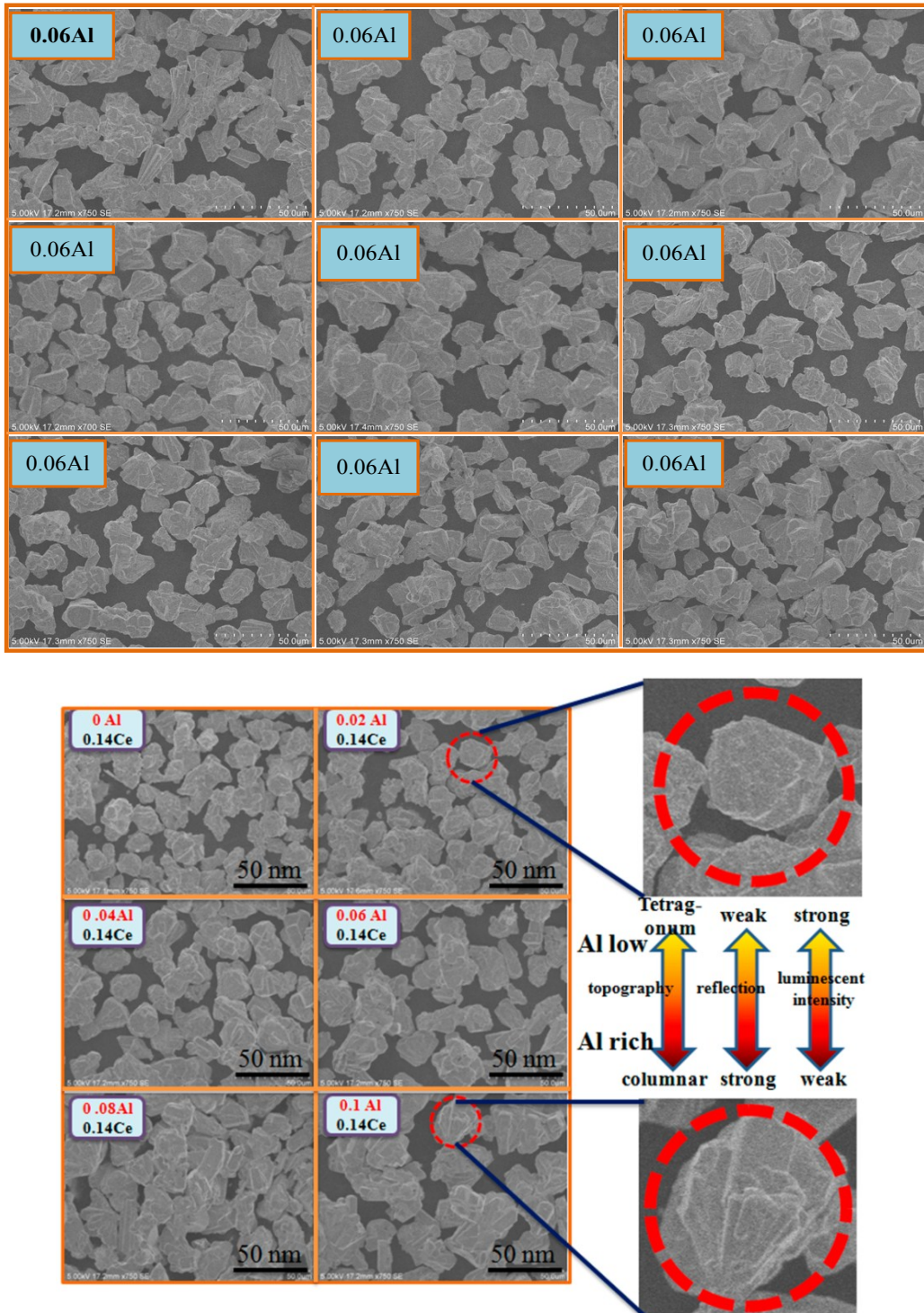


Fig. S2 The SEM image of samples $\text{La}_{3-z}\text{Si}_6\text{N}_{11}:\text{zCe}^{3+}$ and $\text{La}_{3-z}\text{Si}_{5.94}\text{Al}_{0.06}\text{N}_{10.98}:\text{zCe}^{3+}$ ($z = 0.02, 0.06, 0.10, 0.14, 0.18$).

Generally, the luminous efficiency of the phosphor largely depends on the particle morphology, size, crystallinity and crystal structure. The morphology of the $\text{La}_{3-z}\text{Si}_6\text{N}_{11}:\text{zCe}^{3+}$, $\text{La}_{3-z}\text{Si}_{5.94}\text{Al}_{0.06}\text{N}_{10.98}:\text{zCe}^{3+}$ and $\text{La}_{2.86}\text{Si}_{6-x}\text{Al}_x\text{N}_{11-x/3}:\text{0.14Ce}^{3+}$ are

investigated (Figure S2). As shown, with the increase of Al^{3+} doping concentration, the particle size increased and the obvious preferred crystal growth direction of (001) plane. To the right of the graph, shown in Figure 2, the particles are tetragonal when $x = 0.02$, but as x increasing to 0.1, the morphology becoming more columnar and agglomerate. Fig. S3 presents the reflectivity of $\text{La}_{2.86}\text{Si}_{6-x}\text{Al}_x\text{N}_{11-x/3}:0.14\text{Ce}^{3+}$, it is observed that the reflectivity gradually enhanced with the increase of Al^{3+} doping concentration. Normally, nearly spherical particles, well dispersed and crystallinity of the powder are beneficial to the luminous efficiency of phosphor. The above analysis shows that the introduction of Al^{3+} may influence on luminous efficiency of LSN:Ce³⁺.

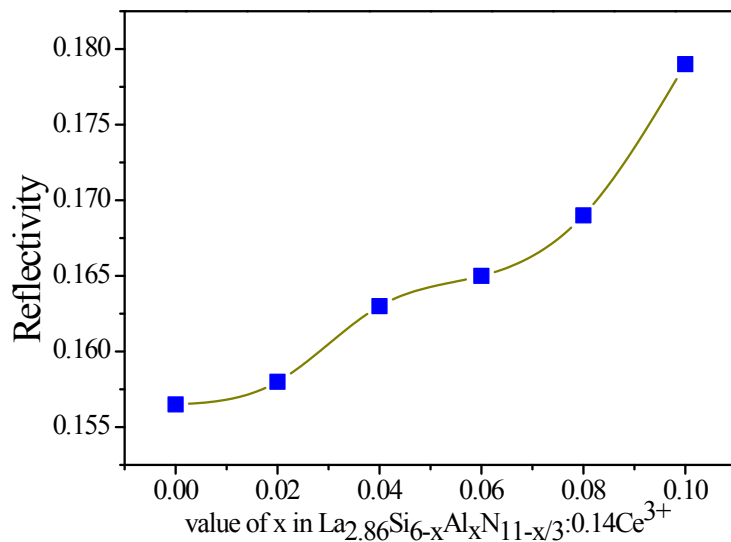


Fig. S3 Reflectivity of $\text{La}_{2.86}\text{Si}_{6-x}\text{Al}_x\text{N}_{11-x/3}:0.14\text{Ce}^{3+}$ ($x = 0, 0.02, 0.04, 0.06, 0.08$ and 0.1) monitored at room temperature.

Fig. S4(a) presents the PL spectra of $\text{La}_{3-z}\text{Si}_6\text{N}_{11}:z\text{Ce}^{3+}$ phosphors under excitation of 445 nm blue light. With an increase of Ce³⁺ dopant concentration, the emission intensity of $\text{La}_{3-z}\text{Si}_6\text{N}_{11}:z\text{Ce}^{3+}$ reached the optimal at $z = 0.14$, and then begin to decrease due to the concentration quenching effect. The emission wavelength shows a

slight red-shift (532 to 535 nm) with increasing concentration of Ce^{3+} , as described in the inset of Fig. S4(a). As literatures^[28-29] report, the red shift of emission peak with the activator concentration increasing attribute to the distance between two activators become shorter ,which resulting the strength of the crystal field splitting. In order to explore the effect of Al^{3+} on the luminescent properties of $\text{La}_3\text{Si}_6\text{N}_{11}:\text{Ce}^{3+}$, on the basis of $\text{La}_{3-z}\text{Si}_6\text{N}_{11}:\text{zCe}^{3+}$, 1% mol($x = 0.06$) Al^{3+} substituting Si^{4+} , the PL spectra were investigated in Fig. S4(b). It is observed that the concentration quenching occurs at $z = 0.10$, which lower than $\text{La}_{3-z}\text{Si}_6\text{N}_{11}:\text{zCe}^{3+}(z = 0.14)$. Moreover, the relative intensity of normalized emission spectra of $\text{La}_{3-z}\text{Si}_{5.94}\text{Al}_{0.06}\text{N}_{10.98}:\text{zCe}^{3+}$ in the range of 580~700 nm gets enhanced and shifted to the longer wavelength region compared with non-doping Al^{3+} while that of the ~535 nm emission were same with $\text{La}_{3-z}\text{Si}_6\text{N}_{11}:\text{zCe}^{3+}$.

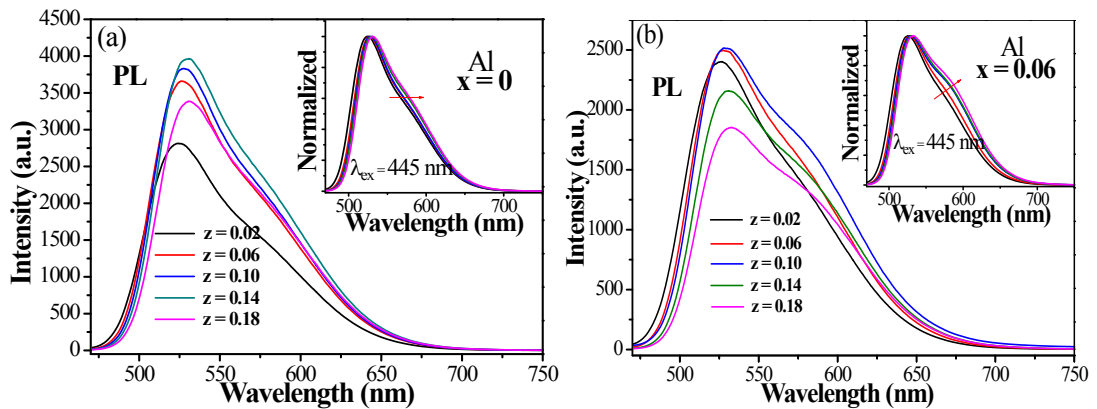


Fig. S4 PL spectra of a series of samples excited at 445 nm, (a) $\text{La}_{3-z}\text{Si}_6\text{N}_{11}:\text{zCe}^{3+}$ ($z = 0.02, 0.06, 0.10, 0.14, 0.18$) (b) $\text{La}_{3-z}\text{Si}_{5.94}\text{Al}_{0.06}\text{N}_{10.98}:\text{zCe}^{3+}$ ($z = 0.02, 0.06, 0.10, 0.14, 0.18$)

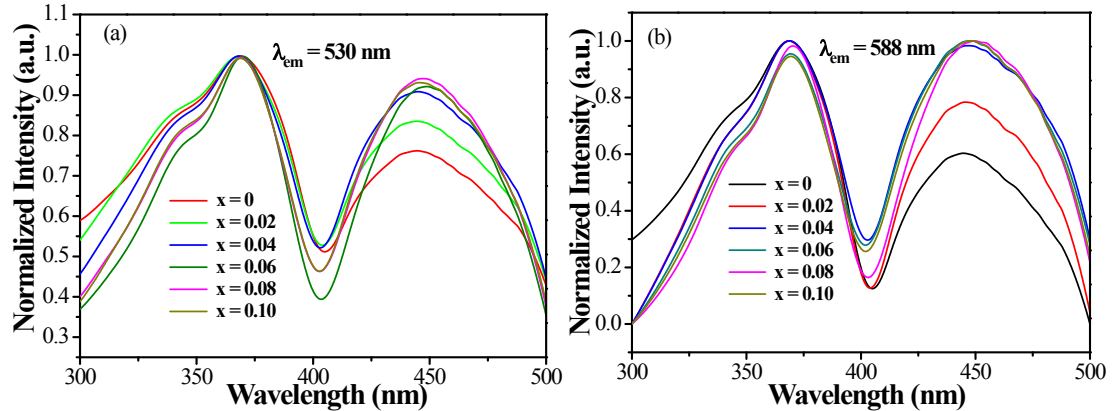


Fig. S5 normalized emission spectra of $\text{La}_{2.86}\text{Si}_{6-x}\text{Al}_x\text{N}_{11-x/3}:0.14\text{Ce}^{3+}$ ($x = 0, 0.02, 0.04, 0.06, 0.08$ and 0.1) monitored at 530 nm(a) and 588 nm(b).

Table S3. The relative emission intensities of $\text{La}_{3-z}\text{Si}_6\text{N}_{11}:z\text{Ce}^{3+}$, $\text{La}_{3-z}\text{Si}_{5.94}\text{Al}_{0.06}\text{N}_{10.98}:z\text{Ce}^{3+}$, $\text{La}_{2.86}\text{Si}_{6-x}\text{Al}_x\text{N}_{11-x/3}:0.14\text{Ce}^{3+}$ and the standard sample BY-201(Mitsubishi Chemical Corporation), carried out using the HAAS-2000 light (Everfine, China).

$\text{La}_{3-z}\text{Si}_6\text{N}_{11}:z\text{Ce}^{3+}$		$\text{La}_{3-z}\text{Si}_{5.94}\text{Al}_{0.06}\text{N}_{10.98}:z\text{Ce}^{3+}$		$\text{La}_{2.86}\text{Si}_{6-x}\text{Al}_x\text{N}_{11-x/3}:0.14\text{Ce}^{3+}$	
Sample	Light	Sample	Light	Sample	Light
BY-201	100.01	BY-201	100.01	$x = 0.02$	91.215
$z = 0.02$	72.304	$z = 0.02$	66.011		
$z = 0.04$	83.886	$z = 0.04$	70.426	$x = 0.04$	72.769
$z = 0.06$	94.977	$z = 0.06$	74.132		
$z = 0.08$	95.824	$z = 0.08$	75.650	$x = 0.06$	63.940
$z = 0.10$	95.817	$z = 0.10$	72.256		
$z = 0.12$	96.486	$z = 0.12$	66.195	$x = 0.08$	55.937
$z = 0.14$	96.829	$z = 0.14$	64.224		
$z = 0.16$	93.482	$z = 0.16$	58.661	$x = 0.10$	41.977
$z = 0.18$	94.030	$z = 0.18$	52.338		

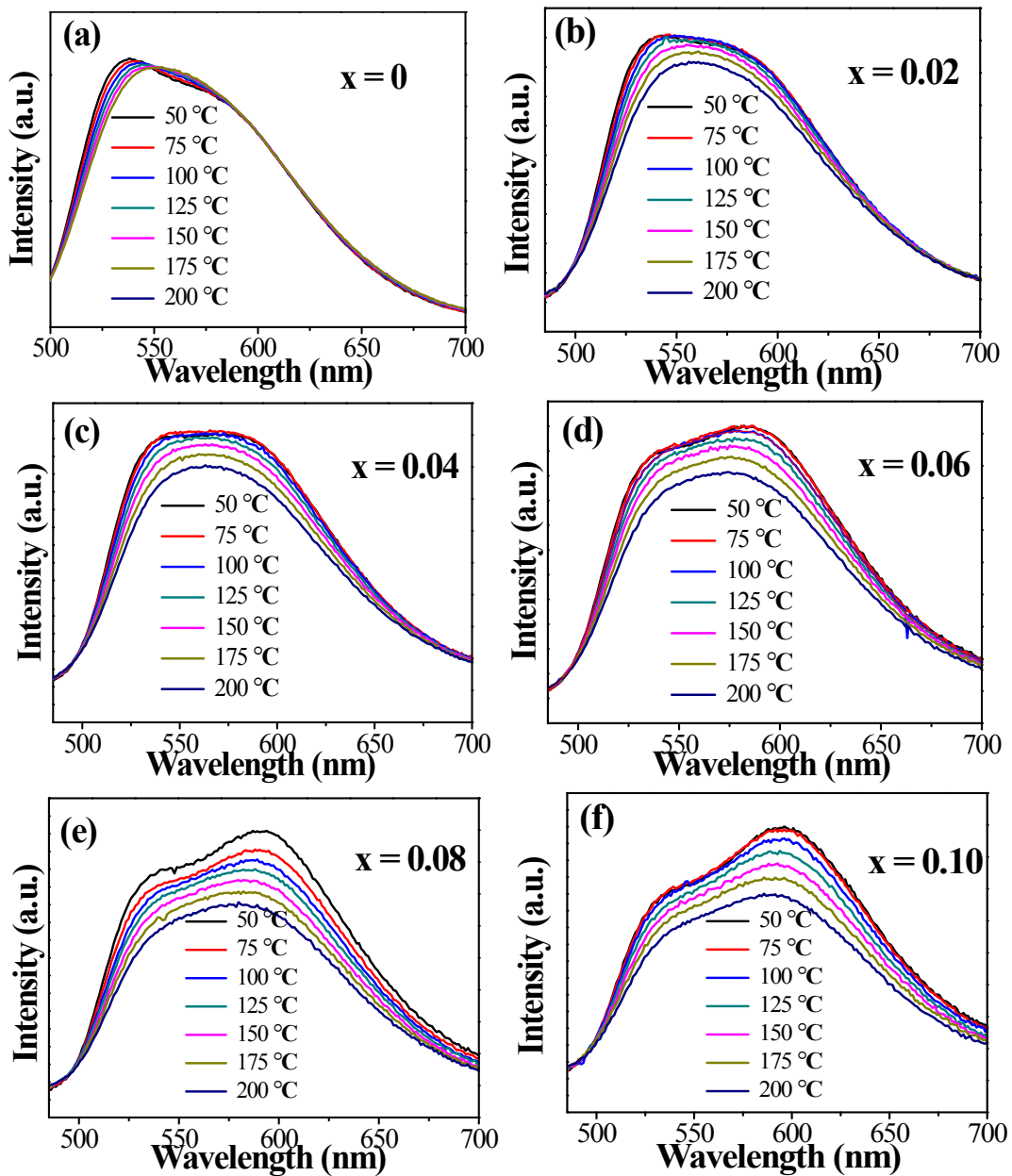


Fig. S6 Temperature-dependent PL spectra of $\text{La}_{2.86}\text{Si}_{6-x}\text{Al}_x\text{N}_{11-x/3}:0.14\text{Ce}^{3+}$ ($x = 0, 0.02, 0.04, 0.06, 0.08$ and 0.1).

x	efficiencies (lm/W)	CIE
0	82.5	(0.42,0.55)
0.02	79.3	(0.42,0.55)

0.04	73.8	(0.44,0.53)
0.06	61.5	(0.49,0.485)
0.08	54.6	(0.488,0.491)
0.1	38.4	(0.495,0.484)

Fig. S7 The CIE and power efficiencies of the white LEDs fabricated with $\text{La}_{2.86}\text{Si}_{6-x}\text{Al}_x\text{N}_{11-x/3}:0.14\text{Ce}^{3+}$ ($x = 0, 0.02, 0.04, 0.06, 0.08$ and 0.1), excited at 460 nm.